

The Persistence and Memory of Polar Nano-Regions in a Ferroelectric Relaxor Under an Electric Field

Guangyong Xu,¹ P. M. Gehring,² and G. Shirane¹

¹Physics Department, Brookhaven National Laboratory, Upton, New York 11973

²NIST Center for Neutron Research, National Institute of Standards and Technology, Gaithersburg, Maryland, 20899

(Dated: June 17, 2018)

The response of polar nanoregions (PNR) in the relaxor compound $\text{Pb}[(\text{Zn}_{1/3}\text{Nb}_{2/3})_{0.92}\text{Ti}_{0.08}]\text{O}_3$ subject to a [111]-oriented electric field has been studied by neutron diffuse scattering. Contrary to classical expectations, the diffuse scattering associated with the PNR persists, and is even partially enhanced by field cooling. The effect of the external electric field is retained by the PNR after the field is removed. The “memory” of the applied field reappears even after heating the system above T_C , and cooling in zero field.

PACS numbers: 77.80.-e, 77.84.Dy, 61.12.Ex

Relaxor ferroelectric materials have garnered enormous attention in the materials science and condensed matter physics communities due to their record-setting dielectric and piezoelectric properties [1]. They have supplanted lead zirconate (PZT) ceramics as the basis of state-of-the-art piezoelectric sensors and actuators that convert between mechanical and electrical forms of energy [2], and they show potential as ferroelectric nonvolatile memories [3]. Compared to classic ferroelectrics, a unique property of relaxors is the appearance of nanometer-sized regions having a local, randomly-oriented polarization at the Burns temperature T_d [4], which is a few hundred degrees above the ferroelectric transition temperature (Curie temperature) T_C . These polar nanoregions (PNR) act like precursors of the spontaneous polarization below T_C , and are believed to play a key role in the unusual relaxor behavior [5]. Several theoretical models based on random fields in a dipole glass [6, 7] have been proposed in order to explain the properties of the PNR. The PNR have been imaged directly with high resolution piezo-response force microscopy [8, 9], while extensive studies have been performed using both neutron [10, 11, 12, 13, 14, 15] and x-ray [16, 17] diffuse scattering techniques. These scattering measurements probe intensities in reciprocal space, which are Fourier transforms of real space structures, and provide valuable information about the magnitudes and orientations of the polarizations of the PNR, their dynamic properties, and the sizes and shapes of the PNR.

There are many unsolved fundamental questions concerning the PNR. Do they facilitate the ferroelectric phase transition of the system, or do they impede it? What prevents them from dissolving into the surrounding, macroscopically polar, environment below the ferroelectric phase transition temperature T_C ? In studies of ferroelectrics, an external field is often applied to monitor how the system responds. Yet few studies have examined the PNR response to an external field. Previous studies [18, 19] have shown that the neutron diffuse scattering measured in directions transverse to the scattering vector can be partially suppressed in relaxor systems by an electric field. In particular the diffuse scattering measured transverse to the (300) Bragg peak in PZN-8%PT is unaffected by an electric field applied along the [001] direction, whereas

that transverse to the orthogonal (003) Bragg peak is significantly suppressed. The anisotropic response of the diffuse scattering in this case seems to suggest that those PNR having “properly oriented” polarizations could be forced to “melt” into the surrounding polar environment with the assistance of an external field, thereby producing a more “microscopically-uniform” polar state.

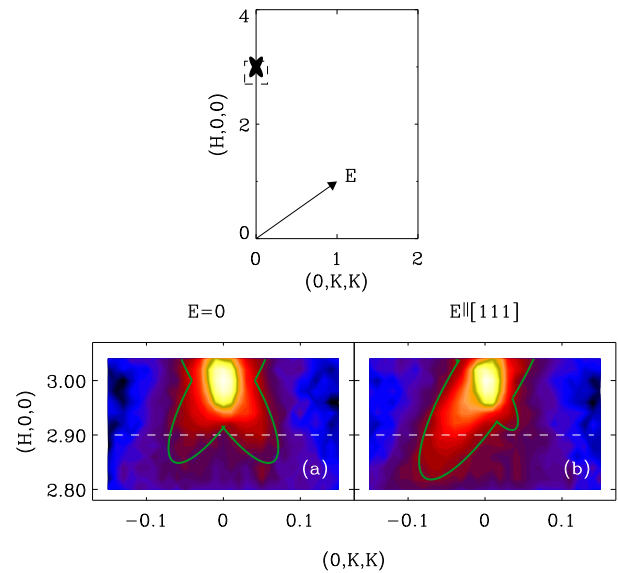


FIG. 1: The top frame is a schematic of the (HKK) reciprocal scattering plane, in which neutron diffuse scattering measurements were performed close to the (300) Bragg peak. The electric field was oriented along [111] as shown by the arrow. The bottom frames show results from measurements made at $T = 300$ K after the sample was zero-field cooled (ZFC) (a) and field-cooled (FC) (b) through T_C . The dashed lines indicate the location of the cuts at $(2.9, K, K)$, shown later in Fig. 2. The solid green lines are guides to the eye to help emphasize the symmetric (a) and asymmetric (b) “butterfly” shapes of the diffuse scattering.

One of the most studied relaxor systems is the lead per-

ovskite $\text{Pb}(\text{Zn}_{1/3}\text{Nb}_{2/3})\text{O}_3$ (PZN). When mixed with PbTiO_3 (PT) to form solid solutions, PZN- x PT single crystals exhibit ultrahigh piezoelectric responses [1, 20]. The piezoelectric property is optimal around $x = 8\%$, which is the PT concentration of the single crystal examined in our study. The zero-field structure [21] and the [001]-oriented electric-field induced structural changes of PZN-8%PT have been studied in detail [22, 23]. The lattice parameter in the cubic phase is $a = 4.045 \text{ \AA}$. Our experimental measurements are then described in terms of reciprocal lattice units (r.l.u.) where $1 \text{ r.l.u.} = a^* = 2\pi/a = 1.553 \text{ \AA}^{-1}$. Because PZN-8%PT has a rhombohedral ground state with $\langle 111 \rangle$ type polarizations at low temperatures, we chose to investigate the effect of an electric field applied along the [111] direction. Contrary to classical expectations, we find that the diffuse scattering does not diminish with the application of an external electric field. Instead, after field cooling, only a part of the diffuse scattering is suppressed in reciprocal space, while another part is markedly enhanced. We also observed interesting “memory” behavior in which the effects of an external field remain after the removal of the field, vanish above $T_C \sim 450 \text{ K}$, and then reappear after zero-field cooling (ZFC) below T_C .

The PZN-8%PT single crystal used in this study was provided by TRS ceramics [24]. The crystal is rectangular in shape, having dimensions $5 \times 5 \times 3 \text{ mm}^3$ with (111), $(\bar{2}11)$, and $(0\bar{1}1)$ surfaces. The Cr/Au electrodes were sputtered onto the top and bottom (111) crystal surfaces. The neutron diffuse scattering measurements were performed with the BT9 triple-axis spectrometer located at the NIST center for Neutron Research. The measurements were made using a fixed incident neutron energy E_i of 14.7 meV, obtained from the (002) reflection of a highly-oriented pyrolytic graphic (HOPG) monochromator, horizontal beam collimations of 40° - 40° - 40° - 80° , and the (002) reflection of an HOPG analyzer to fix the energy of the scattered neutron beam. The sample was oriented with the $(0\bar{1}1)$ surface facing vertically. The scattering plane is therefore the (HKK) plane, which is defined by the two primary vectors [100] and [011]. The [111] electric field direction lies in the horizontal scattering plane.

Ideally, diffuse scattering intensities should be measured around different $\{111\}$ peaks to gauge the net effect of a [111]-oriented electric field. However, the neutron diffuse scattering is very weak around all of the $\{111\}$ peaks due to a small neutron scattering structure factor [13]. Instead, the measurements were performed near the (300) Bragg peak, where the diffuse scattering is strong, and the Bragg peak intensity is weak, as shown schematically in the top frame of Fig. 1. Because of limitations on the maximum achievable scattering angle, we were only able to measure the lower half ($H \leq 3$) of the butterfly-pattern. The data obtained at $T = 300 \text{ K}$ ($< T_C \approx 440 \text{ K}$ in zero field) are shown in the bottom frame of Fig. 1. When the crystal is zero-field cooled (ZFC), the diffuse scattering pattern is symmetric about the [100] axis, and forms the butterfly-shape with “wings” of equal intensity on each side shown in Fig. 1 (a). This pattern is consistent with the three-dimensional diffuse scattering dis-

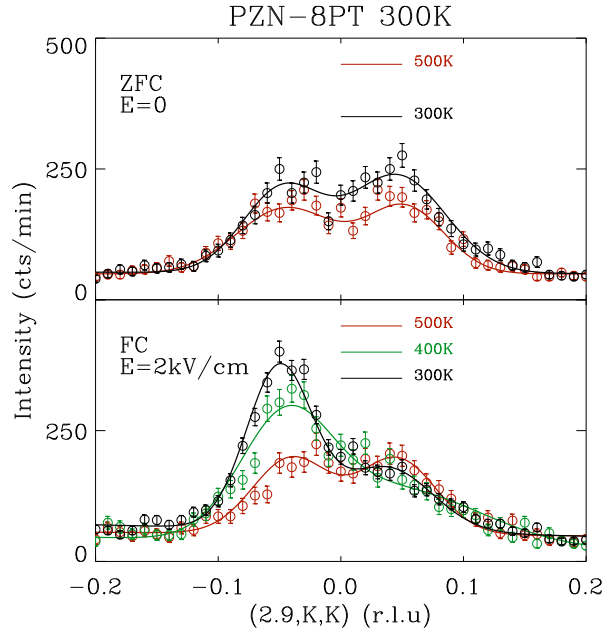


FIG. 2: Linear scans performed at $(2.9, K, K)$, for the ZFC state (top panel), and the FC state (bottom panel), measured at different temperatures. The solid lines are fits to a sum of two Gaussian peaks.

tribution consisting of $\langle 110 \rangle$ rod-type intensities reported in Ref. 25, where PNR with different polarizations contribute to different $\langle 110 \rangle$ diffuse rods. Because of the non-zero out-of-plane wavevector resolution of our measurements, the tails of the $\langle 110 \rangle$ rods are picked up when scanning away from the center of the Bragg peak in the (HKK) plane. This results in the butterfly-shaped pattern, which (neglecting the Q^2 factor in the diffuse intensity) is symmetric about the wavevector $Q=(3,0,0)$, as required by the crystal symmetry.

After zero-field cooling to $T = 300 \text{ K}$ (below T_C) we applied a moderate electric field $E = 2 \text{ kV/cm}$ along the [111] direction. No change in the diffuse scattering was observed, suggesting that the PNR are robust against an external field in the ferroelectric phase. The sample was then heated to $T = 500 \text{ K}$, and an electric field of $E = 2 \text{ kV/cm}$ along [111] was reapplied. No changes were evident at this temperature as a result of the field. However, after field-cooling through T_C ($\approx 460 \text{ K}$ for $E = 2 \text{ kV/cm}$) back to $T = 300 \text{ K}$, the diffuse scattering pattern developed a strong asymmetry about the [100] direction as shown in Fig. 1 (b). The left wing is clearly enhanced while the right one is suppressed. A more detailed look at the temperature dependence of the diffuse scattering is provided in Fig. 2. Here characteristic linear scans of the diffuse scattering intensity measured along $(2.9, K, K)$ (see the dashed line in Fig. 1) are plotted. In the ZFC state the symmetric double-peaked profiles indicate that the intensities from both wings increase equally with cooling. In the FC state, for which the [111]-oriented E -field was initially applied at $T = 500 \text{ K}$ in the cubic (paraelectric) phase, it is only after cooling below T_C that the intensity of the left

tern observed in the FC state can be explained by a simple model. Knowing that the diffuse scattering consists of $\langle 110 \rangle$ rods [25], we can see that the lower left wing of the butterfly shown in Fig. 1 (a) originates from the tails of rods of diffuse scattering intensity oriented along the $[110]$ and $[101]$ directions, and the lower right wing originates from the tails of rods oriented along the $[1\bar{1}0]$ and $[10\bar{1}]$ directions. More importantly, the polarizations of PNR contributing to different $\langle 110 \rangle$ diffuse rods have also been clearly identified to point along the perpendicular $\langle 1\bar{1}0 \rangle$ directions [25]. Therefore, the enhanced left wing observed in our measurements arises from PNR with polarizations along $[1\bar{1}0]$ and $[10\bar{1}]$, both perpendicular to the external $[111]$ electric field, and the suppressed right wing arises from PNR with polarizations along $[110]$ and $[101]$, which are not perpendicular to the field. There are then two possible scenarios that can lead to the enhancement of PNR with polarizations perpendicular to the field. The first is one in which the PNR are affected directly by the field so that those PNR having perpendicular polarizations are more favored by the FC process. This is quite unlikely since the electric field tends to align electric dipole moments along the field direction. The second is one in which the PNR are not affected directly by the external field. In the paraelectric phase, they can have polarizations that point along any one of the six $\langle 110 \rangle$ directions and the field has no effect. In the low temperature ferroelectric phase, however, the six $\langle 110 \rangle$ directions are no longer equivalent. The PNR may tend to grow with polarizations perpendicular to the $\langle 111 \rangle$ type polarization of the surrounding lattice. This actually prevents them from merging into the surrounding polar lattice. The electric field only affects the alignment of the ferroelectric domains in which the PNR are embedded, so that the enhancement of perpendicular PNR can be observed at a macroscopic level. This model is purely speculative, and more experimental support is required to confirm or refute it. However its simplicity can be appreciated as a starting point for developing an understanding of PNR behavior.

After removal of the field, the effect on the crystal remains, and so will the configuration of the PNR. However we do not currently understand the reason for the “memory” effect, where heating to $T_C < T < T_R$ does not “depole” the system. The memory of the electric field is only hidden, and reappears again when zero-field cooled below T_C . Considering the case of magnetic systems with random fields, the effect of an external magnetic field can lead to very different behaviors, even a change of T_C , between FC and ZFC [29]. There nonequilibrium effects play an essential role. In relaxor systems, similar random-field models for a dipole glass can be considered. Based on our measurements of the structural changes [24], $T_C \sim 460$ K for $E = 2$ kV/cm was only slightly higher than $T_C \sim 440$ K for $E = 0$ kV/cm. However, the electric field may also have effects on some other hidden degrees of freedom that do not fully dissolve at T_C , and therefore are not directly observable in structural measurements. For example, one such possibility is that the effect of the electric field may be “remembered” by the lattice dynamics, i. e., atomic mo-

tions associated with the PNR. Even when the whole system goes into a paraelectric phase above T_C , the memory of the previous configuration could be embedded within the atomic motions in a metastable phase at $T_C < T < T_R$. The system may not be able to equilibrate over experimentally accessible time scales. These hidden effects could resurface again upon cooling and produce the spontaneous “repoling”. The results we have reported here also have significant application implications in areas such as ferroelectric memory devices. An electric field can be used to embed information in the relaxor system. After removing the field, the information will only surface for $T < T_C$, but can not be erased unless heating the system up to $T > T_R$, making the device useful for temperatures in the neighborhood of T_C , where the various relaxor properties are optimal.

We would like to thank C. Broholm, H. Hiraka, S. M. Shapiro, C. Stock, J. M. Tranquada, and Z. Zhong, for stimulating discussions. Financial support from the U.S. Department of Energy under contract No. DE-AC02-98CH10886 is also gratefully acknowledged.

-
- [1] S.-E. Park and T. R. Shroud, *J. Appl. Phys.* **82**, 1804 (1997).
 - [2] K. Uchino, *Piezoelectric actuators and ultrasonic motors* (Kluwer Academic, Boston, 1996).
 - [3] B. H. Park, B. S. Kang, S. D. Bu, T. W. Noh, J. Lee, and W. Jo, *Nature* **401**, 682 (1999).
 - [4] G. Burns and F. H. Dacol, *Phys. Rev. B* **28**, 2527 (1983).
 - [5] L. E. Cross, *Ferroelectrics* **76**, 241 (1987).
 - [6] R. Pirc and R. Blinc, *Phys. Rev. B* **60**, 13470 (1999).
 - [7] R. Fisch, *Phys. Rev. B* **67**, 094110 (2003).
 - [8] P. Lehnen, W. Kleemann, T. Woike, and R. Pankrath, *Phys. Rev. B* **64**, 224109 (2001).
 - [9] V. V. Shvartsman and A. L. Kholkin, *Phys. Rev. B* **69**, 014102 (2004).
 - [10] S. B. Vakhrushev, A. A. Naberezhnov, N. M. Okuneva, and B. N. Savenko, *Phys. Solid State* **37**, 1993 (1995).
 - [11] K. Hirota, Z.-G. Ye, S. Wakimoto, P. M. Gehring, and G. Shirane, *Phys. Rev. B* **65**, 104105 (2002).
 - [12] Guangyong Xu, G. Shirane, J. R. D. Copley, and P. M. Gehring, *Phys. Rev. B* **69**, 064112 (2004).
 - [13] H. Hiraka, S.-H. Lee, P. M. Gehring, Guangyong Xu, and G. Shirane, *Phys. Rev. B* **70**, 184105 (2004).
 - [14] J. Hlinka, S. Kamba, J. Petzelt, J. Kulda, C. A. Randall, and S. J. Zhang, *J. Phys.: Condens. Matter* **15**, 4249 (2003).
 - [15] S. N. Gvasaliya, S. G. Lushnikov, and B. Roessli, *Phys. Rev. B* **69**, 092105 (2004).
 - [16] H. You and Q. M. Zhang, *Phys. Rev. Lett.* **79**, 3950 (1997).
 - [17] N. Takesue, Y. Fujii, and H. You, *Phys. Rev. B* **64**, 184112 (2001).
 - [18] S. B. Vakhrushev, A. A. Naberezhnov, N. M. Okuneva, and B. N. Savenko, *Phys. Solid State* **40**, 1728 (1998).
 - [19] P. M. Gehring, K. Ohwada, and G. Shirane, *Phys. Rev. B* **70**, 014110 (2004).
 - [20] J. Kuwata, K. Uchino, and S. Nomura, *Jpn. J. Appl. Phys.* **21**, 1298 (1982).
 - [21] B. Noheda, D. E. Cox, and G. Shirane, *Ferroelectrics* **267**, 147 (2002).
 - [22] K. Ohwada, K. Hirota, P. W. Rehrig, Y. Fujii, and G. Shirane,

- Phys. Rev. B **67**, 094111 (2003).
- [23] B. Noheda, Z. Zhong, D. E. Cox, G. Shirane, S.-E. Park, and P. Rehrig, Phys. Rev. B **65**, 224101 (2002).
- [24] For this particular sample, the structure and therefore the phase diagram was determined by monitoring the intensity and splitting of (200), (022) and (111) Bragg peaks using elastic neutron scattering techniques. All measurements were performed with cooling processes. In zero external field $T_C \approx 440$ K for the transition from cubic to tetragonal symmetry, and $T_{C2} \approx 340$ K for the transition from tetragonal to rhombohedral symmetry. Under an external electric field $E = 2$ kV/cm oriented along the [111] direction, $T_C \approx 460$ K, slightly higher than the zero-field value. $T_{C2} \approx 340$ K does not change much under field.
- [25] Guangyong Xu, Z. Zhong, H. Hiraka, and G. Shirane, Phys. Rev. B **70**, 174109 (2004).
- [26] K. H. Fisher and J. A. Hertz, *Spin Glasses* (Cambridge University Press, Cambridge, 1991).
- [27] F. Cordero, F. Craciun, A. Franco, D. Piazza, and C. Galassi, Phys. Rev. Lett. **93**, 097601 (2004).
- [28] T. Granzow, T. Woike, M. Wöhlecke, M. Imlau, and W. Kleemann, Phys. Rev. Lett. **89**, 127601 (2002).
- [29] R. J. Birgeneau, J. Magn. Magn. Mater. **177**, 1 (1998).